JACS
JOURNAL OF THE AMERICAN CHEMICAL SOCIETY

Article

pubs.acs.org/JACS

Reversible Modulation of DNA-Based Hydrogel Shapes by Internal Stress Interactions

Yuwei Hu,[†] Jason S. Kahn,[†] Weiwei Guo,[†] Fujian Huang,[†] Michael Fadeev,[†] Daniel Harries,[†,‡] and Itamar Willner*[,†]

[†]Institute of Chemistry and The Center for Nanoscience and Nanotechnology and [‡]The Fritz Haber Research Center, The Hebrew University of Jerusalem, Jerusalem 91904, Israel

Supporting Information

ABSTRACT: We present the assembly of asymmetric two-layer hybrid DNA-based hydrogels revealing stimuli-triggered reversibly modulated shape transitions. Asymmetric, linear hydrogels that include layer-selective switchable stimuli-responsive elements that control the hydrogel stiffness are designed. Trigger-induced stress in one of the layers results in the bending of the linear hybrid structure, thereby minimizing the elastic free energy of the systems. The removal of the stress by a counter-trigger restores the original linear bilayer hydrogel. The stiffness of the DNA hydrogel layers is controlled by thermal, pH (i-motif), K^+ ion/crown ether (G-quadruplexes), chemical (pH-doped polyaniline), or biocatalytic (glucose oxidase/urease) triggers. A theoretical model relating the experimental bending radius of curvatures of the hydrogels with the Young's moduli and geometrical parameters of the hydrogels is provided. Promising applications of shape-regulated stimuli-responsive asymmetric hydrogels include their use as valves, actuators, sensors, and drug delivery devices.

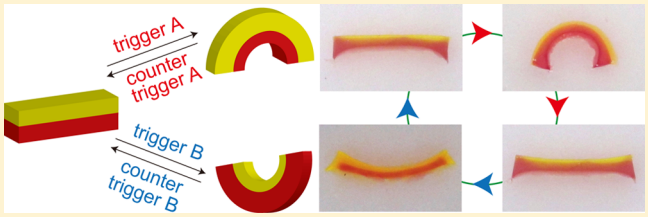

INTRODUCTION

Substantial experimental[1] and theoretical[2] research efforts are directed to the development of signal-triggered shape transitions of soft hydrogel polymer matrices and to the understanding of the physical mechanisms governing the structural transitions (bending or twisting) of the hydrogels. Interest in shape-adaptive materials originates from the fact that the hydrogel systems mimic stimuli-responsive biomechanical processes,[3] such as seedpod distribution or morphogenesis, and from their potential in biomedical device applications,[4] soft robotics,[5] optical devices,[6] microfluidic devices,[7] and responsive surface coatings.[8] Different signals, such as temperature,[9] pH,[10] light,[11] electric,[12] and solvent-induced swelling or shrinkage of the matrices,[13] were used to stimulate reversible structural transitions of the polymer hydrogels. Ingenious methods to pattern stimuli-responsive hydrogels and to engineer localized stress changes in the matrices were implemented to develop programmed three-dimensional hydrogels[14] and to induce directional surface motility of the structures.[15]

The structural and functional information encoded in nucleic acids has been extensively used to develop DNA switching systems,[16] such as DNA machines,[17] DNA-nanoparticle hybrids for sensing,[18] switchable catalytic nucleic acids (DNAzymes),[19] switchable drug carriers (SiO_2 nanoparticles, microcapsules),[20] switchable nanocontainers for programmed synthesis,[21] and programmed aggregation/deaggregation of semiconductor quantum dots for switchable chemiluminescence resonance energy transfer (switchable CRET).[22] Specifically, stimuli-responsive DNA-based hydrogels undergoing cyclic hydrogel-to-liquid transitions were reported.[23] Different stimuli, such as pH,[24] metal ion/ligand,[25] strand/antistrand,[26] and light,[27] were used to stimulate reversible hydrogel-to-solution phase transitions. Different applications of stimuli-responsive DNA-based hydrogels were suggested, including controlled drug delivery,[28] controlled transport through pores,[29] and functional materials for sensing[30] or actuator[27] operations. Furthermore, our laboratory introduced the use of DNA-functionalized polymer hydrogels cross-linked by two different trigger-addressable nucleic acid bridges that allowed the construction of hydrogels of controlled stiffness as bulk material[24c,25,26] and on surfaces.[31] These stimuli-responsive matrices were used by us to develop shape-memory hydrogels[24,26] and functional coatings on electrodes for switchable electrocatalysis.[31]

Stimuli-controlled mechanical changes of biomaterials are important in nature, e.g., disposal of seeds from seedpods by humidity or temperature triggers.[32] Substantial research efforts have been directed in recent years to mimic such processes by synthetic materials.[33] Ingenious asymmetric polymer matrices that allowed the dictated introduction of stress into the polymer material by external triggers, e.g., temperature or electrical stimuli, allowed the programmed mechanical control of the shapes of the composites. Important theoretical modeling of the stimuli-controlled shapes of the structures was introduced,[34] and different applications of stimuli-responsive mechanically modulated structures of such polymers were suggested, including the design of electro-actuators or switches.[9d,33b,35] The ability to reversibly control the stiffness of

Received: October 5, 2016
Published: November 16, 2016

DOI: 10.1021/jacs.6b10458
J. Am. Chem. Soc. 2016, 138, 16112−16119

DNA-based hydrogels by diverse external stimuli provides a rich "tool-box" to design asymmetric hydrogel structures of stimuli-responsive hydrogel domains of controlled stiffness. Such hydrogel structures could provide the basis for the assembly of DNA hydrogel materials that reveal signal-triggered mechanically modulated structures. In the present study, we introduce the novel application of stimuli-responsive DNA hydrogels as functional matrices for the mechanically-dictated shape bending of the hydrogel. We demonstrate the assembly of the asymmetric stimuli-responsive bilayer DNA-based hydrogel composites. We reveal that the dictated mechanical stiffness and contraction/expansion introduced into addressed domains of the bilayer hydrogel matrix leads to controlled bending of the hydrogel. Temperature- and pH-stimulated formation and dissociation of DNA i-motif and K^+ ion/crown ether formation and dissociation of G-quadruplexes act as triggers that control the stiffness of the hydrogel domains. The experimental bending parameters are theoretically modeled, and excellent agreement between the experimental and calculated stimuli-triggered shapes is obtained. Furthermore, we demonstrate that the asymmetric, chemically catalyzed deposition of polyaniline on the hydrogel composite enhances the stiffness of a hydrogel domain in the bilayer hybrid structure, resulting in its bending. The polyaniline matrix undergoes reversible pH-stimulated doping/undoping reactions that result in cyclic and reversible shape transitions. Lastly, the incorporation of two enzymes (glucose oxidase and urease) into the bilayer hybrid structure of two hydrogels results in selective i-motif-induced stress in one of the hydrogels, leading to reversible shape transitions upon the glucose oxidase-biocatalyzed acidification of the system in the presence of glucose and the urease-biocatalyzed neutralization of the system in the presence of urea, respectively. The results highlight the broad scope of stimuli-responsive DNA-based hydrogels for the mechanical control of the shape of the materials. The different systems introduce promising new applications of the materials as sensors, actuators, or biomedical systems.

RESULTS AND DISSCUSSION

In order to induce the triggered shape transitions (bending) of DNA hydrogel systems, we constructed nonuniform bilayered hybrid constructs, where one of the layers includes a stimuli-responsive element that controls the switchable stiffness of the layer. Alternatively, either of the two layers is modified with a different stimuli-responsive trigger that allows the addressable triggering of the respective layers. Figure 1 depicts the concept of the assembly of the two-layer DNA-based asymmetric hybrid structure for the modulated bending of the hydrogels. A polyacrylamide-type hydrogel cross-linked by the T−A·T triplex motif, which could be separated into a T−A duplex and a single-strand T by changing the hydrogel pH from 7.0 to 10.0, is assembled as the first layer in the mold, which is then changed back to pH 7.0 to form the hydrogel I. This hydrogel matrix includes a stimuli-responsive element A, that in the presence of the appropriate trigger, controls the switchable and reversible properties of the hydrogel I layer. The second acrylamide-type hydrogel is similarly cross-linked by the T−A·T triplex, and it includes a different encoded triggering element B that allows the cyclic switchable control of the stiffness of the hydrogel, hydrogel II. Changing the hydrogel II from neutral to pH 10.0 separates the T−A·T triplex cross-linking units and it transforms to a solution state, which is added onto the hydrogel I deposited in the mold. The basic hydrogel II solution

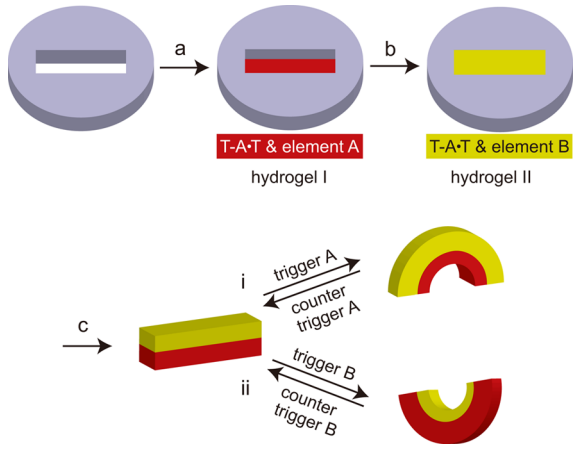

Figure 1. Schematic preparation of an asymmetric bilayered hydrogel hybrid in a mold (a, b), its extrusion (c), and its triggered bending by controlling the reversible stress in one of the hydrogel layers.

dissociated the boundary between hydrogel I and the hydrogel II solution, and upon pH neutralization of the system, self-healing of the two hydrogels I and II proceeds, leading to a hybrid structure stabilized by common T−A·T bridges. The bilayer construct of hydrogels I and II is then extracted from the mold. Activation of trigger A, associated with hydrogel I to yield a hydrogel of increased stiffness, results in a stress in the bilayer composite that induces the bending of the linear hybrid into a curved structure that neutralizes the stress interactions by adjusting the respective lengths/widths of the two hydrogels, path i. Similarly, the addressed activation of stiffness of hydrogel II by stimulus B results in the bending of the hybrid structure into an oppositely curved shape, path ii. By the cyclic application of the stiffening signals, the respective hybrids are switched between curved and linear structures, respectively.

Figure 2a depicts the simplest thermally controlled bending of the hybrid bilayer hydrogel consisting of T−A·T-bridged [(**1**)/(**2**)/(**1**)], nonresponsive polyacrylamide hydrogel I (yellow) and the T−A·T-cross-linked, thermosensitive poly-*N*-isopropylacrylamide (pNIPAM) hydrogel II (red). While at 25 °C the bilayer hydrogel retains a linear hybrid structure, but heating the system to 45 °C rigidifies the pNIPAM hydrogel due to the gel-to-solid transition, resulting in the bending of the composite structure. Cooling the system leads to the reverse solid-to-gel transition, resulting in the reversible and switchable regeneration of the linear bilayer configuration (Figure 2b). The degree of bending curvature is controlled by the thickness/length of the bilayer hybrid [Figure S1, Supporting Information (SI)]. The time-dependent thermally induced bending of the linear-to-curved shape, and the reverse process upon cooling of the curved structure to 25 °C are shown in Figure S2 (SI). Also, by self-healing of two linear bilayer hydrogels linked together with opposite directionalities of the hydrogels, reversible transitions between linear and wave-shaped structures are demonstrated (Figure S3, SI). The assembly of a bifunctional triggered two-layer hydrogel system, revealing addressable bending directionalities, is depicted in Figure 2c,d. Hydrogel II consists of the thermosensitive T−A·T-cross-linked [(**1**)/(**2**)/(**1**)] pNIPAM hydrogel (red), and the second T−A·T-bridged hydrogel layer (yellow), hydrogel III, includes cytosine-rich tethers [(**3**)] that correspond to half of the i-motif sequence. At pH 7.0 and at 25 °C, the linear bilayer hydrogel structure is generated. Treatment of the hybrid hydrogel at pH

DOI: 10.1021/jacs.6b10458
J. Am. Chem. Soc. 2016, 138, 16112−16119

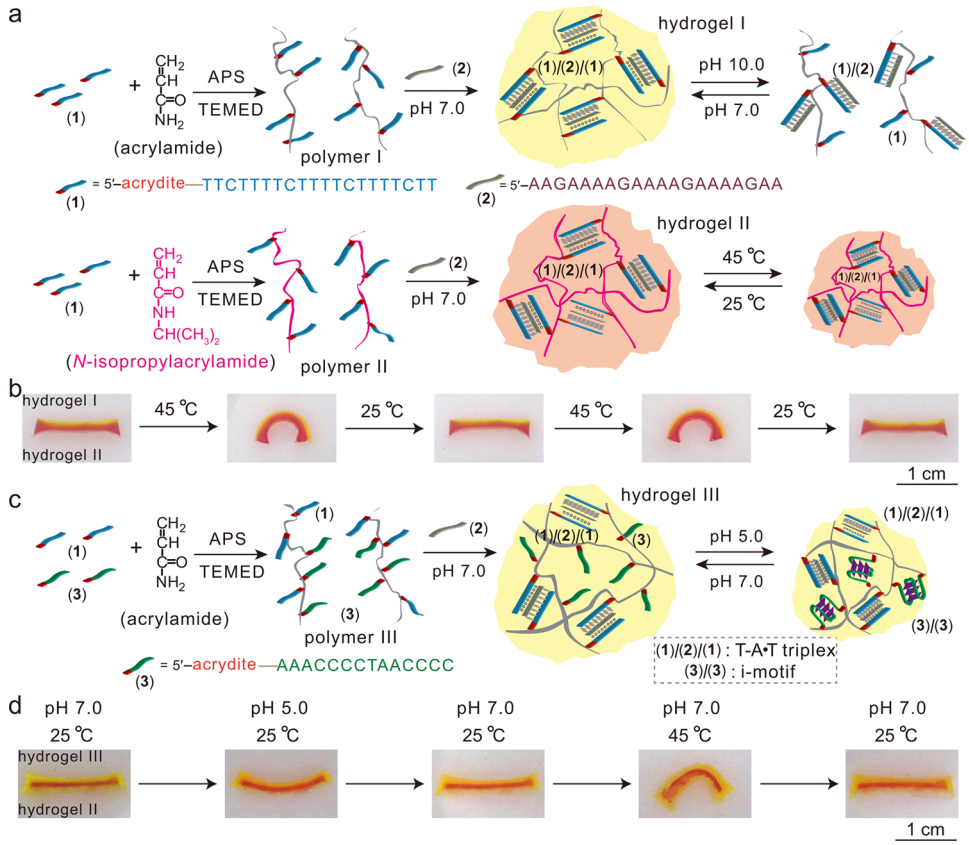

Figure 2. Reversible and switchable shape transitions of a hybrid hydrogel by pH or thermal stimuli: (a) Synthesis of an acrylamide copolymer hydrogel consisting of acrydite T−A·T-cross-linked acrylamide chains (yellow) and of a pNIPAM copolymer composed of acrydite T−A·T-cross-linked pNIPAM chains (red). The T−A·T-cross-linked hydrogel undergoes reversible pH-stimulated gel-to-liquid transitions at pH 10.0 or 7.0, and the thermally-induced, reversible gel-to-solid transitions are shown, respectively. (b) Thermally induced shape transitions of the bilayered hydrogel hybrid consisting of hydrogels I and II. (c) Synthesis of an acrylamide copolymer hydrogel (hydrogel III) composed of acrylamide units and acrydite i-motif subunits and cross-linked by acrydite T−A·T triplex bridges. The hydrogel undergoes reversible pH-stimulated transitions between a less-stiff hydrogel at pH 7.0 and a hydrogel of enhanced stiffness being cooperatively cross-linked at pH 5.0 by the T−A·T and i-motif bridges. (d) Triggered pH-induced and thermally stimulated shape transitions of a bilayered asymmetric hybrid composed of hydrogels II and III.

5.0 (25 °C) triggers the formation of the i-motif bridging units in hydrogel III. The enhanced cross-linking of hydrogel III results in increased stiffness and induces a stress in the composite. This leads to a positive bending of the bilayer. Neutralization of the system to pH 7.0 regenerates the linear structure. Further heating of the linear composite leads to the gel-to-solid transition of the pNIPAM hydrogel (hydrogel II), which results in a stress that leads to the negative bending of the composite. The further cooling of the system to 25 °C restores the linear shape of the bilayer hydrogel, demonstrating the reversible and cyclic control of the shapes of the bilayer hydrogel by pH and thermal stimuli (Figure 2d). The similar bidirectional bending of the bilayer hydrogel system has been demonstrated by combining the T−A·T-cross-linked, thermosensitive pNIPAM hydrogel (hydrogel II) with the T−A·T-cross-linked hydrogel IV, which includes guanosine-rich tethers [(**4**)] that are capable of self-assembling into the K^+ ion-stabilized G-quadruplex (Figure S4, SI).

In addition, an asymmetric bilayer hydrogel structure undergoing, in the presence of appropriate triggers, cyclic and reversible shape transitions across five different states was constructed (Figure 3). Hydrogel IV is composed of the T−A·T-cross-linked polyacrylamide chains that were functionalized with the guanosine-rich tethers [(**4**)], which correspond to the half-subunits of a K^+ ion-stabilized G-quadruplex (Figure 3a). Hydrogel V consists of the T−A·T-cross-linked pNIPAM polymer chains that are also functionalized with cytosine-rich tethers [(**3**)], which correspond to half-subunits of the i-motif structure (that is stabilized at pH 5.0) (Figure 3b). The triggered shape transitions of the bilayer hydrogel are depicted in Figure 3c. At pH 7.0 and 25 °C, and in the absence of K^+ ions, the hybrid bilayer hydrogel exists in a linear configuration, state i (since no i-motif or G-quadruplex can be formed). Heating the system to 45 °C induces the gel-to-solid transition of the pNIPAM hydrogel, and the resulting stress leads to a negative bending of the bilayer shape, state ii. The subsequent cooling of the system to 25 °C restores state i. Further treatment of the bilayer hydrogel at 25 °C and at pH 5.0 results in the cooperative cross-linking of the pNIPAM hydrogel, by the formation of i-motif structures, and the resulting stress induces a negative bending, state iii. Further heating of the hydrogel to 45 °C enhances the negative bending, due to the hydrogel-to-solid transition, state ii + iii. Note that due to the cooperative stress developed in the system by the i-motif and solidification of the pNIPAM hydrogel, an enhanced negative bending radius of curvature is observed as compared to state ii (0.40 vs 0.47 cm). Cooling the bent structure, state ii + iii, to 25 °C restores state iii, and neutralization of state iii, pH 7.0, at 25 °C, regenerates the linear bilayer configuration, state i. Subjecting state i to K^+ ions results in the cooperative cross-

DOI: 10.1021/jacs.6b10458
J. Am. Chem. Soc. 2016, 138, 16112−16119

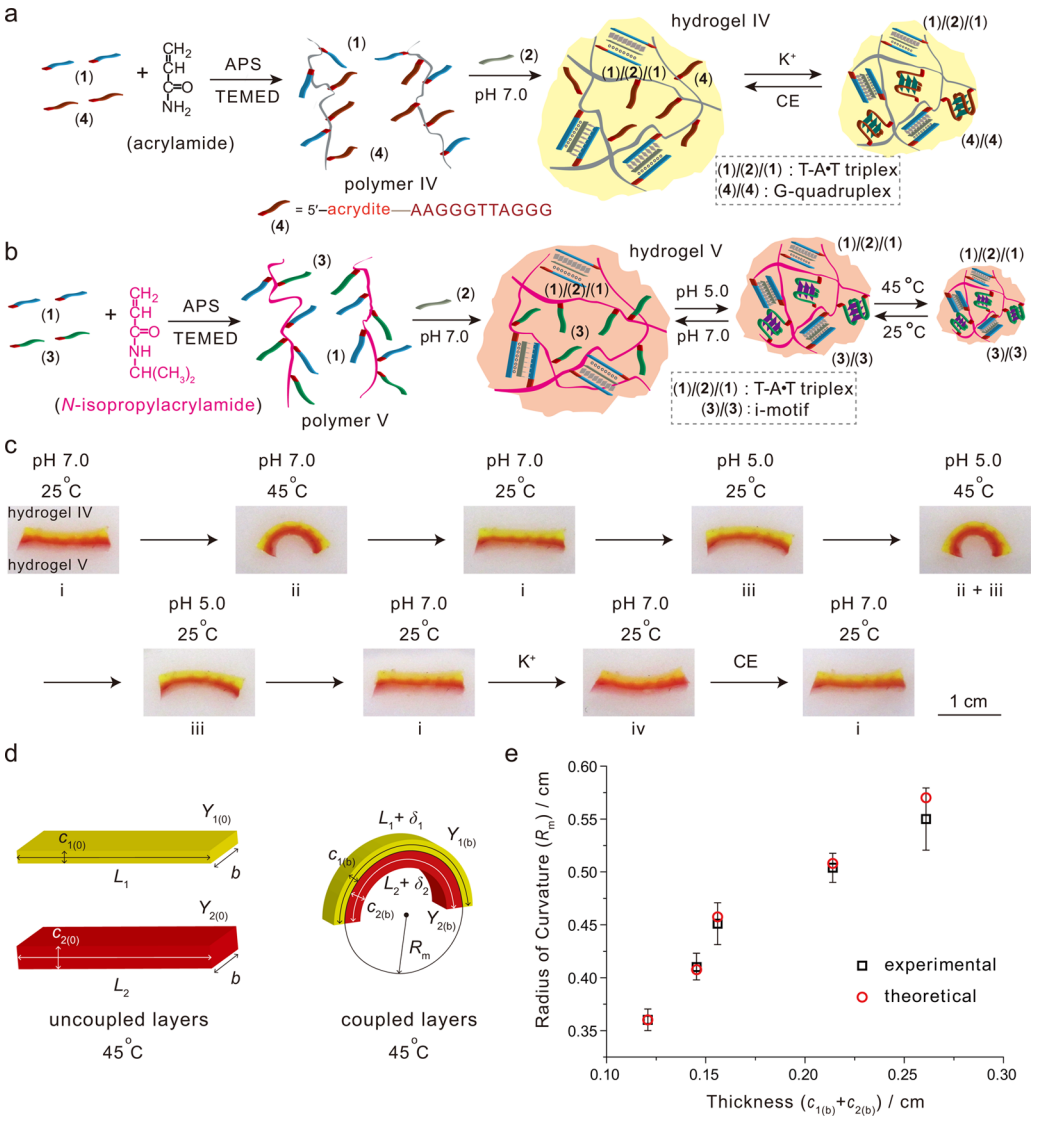

Figure 3. Reversible and switchable shape transitions of a bilayered hybrid hydrogel using three different triggers: K^+ions/crown ether, pH, and temperature. (a) Synthesis of hydrogel IV consisting of an acrylamide copolymer composed of acrylamide units and acrydite G-quadruplex units, cross-linked by acrydite T−A·T bridges. The hydrogel undergoes reversible and switchable transitions between a less-stiff and stiff hydrogel state, bridged cooperatively by the T−A·T bridges and K^+ ion-stabilized G-quadruplex using K^+ ions and crown ether as triggers. (b) Synthesis of hydrogel V composed of *N*-isopropylacrylamide units and acrydite i-motif subunits and cross-linked by the acrydite T−A·T bridges. The hydrogel undergoes reversible hydrogel transitions between a less-stiff hydrogel and a hydrogel of enhanced stiffness, via cooperative cross-linking by i-motif and T−A·T bridges and thermally induced hydrogel-to-solid transitions. (c) Cyclic and reversible shape transitions upon subjecting the bilayered hybrid composed of hydrogels IV and V to three different triggers: K^+ ions/crown ether, pH, and temperature. (d) Geometrical and stiffness parameters associated with the bilayer hydrogel components and with the stimuli-responsive bent shape of the hybrid hydrogel. (e) Experimental vs theoretical radius of curvatures of the shaped hydrogel I, hydrogel II and hydrogel IV/hydrogel V hybrid composites, subjected to the temperature trigger, as a function of the geometrical and stiffness features of the two hydrogels. (Error bars for the experimental radius of curvature are derived from $N = 4$ experiments.)

linking of hydrogel IV by K^+ ion-stabilized G-quadruplex bridges, leading to a positive bending of the hybrid hydrogel, state iv. The subsequent treatment of the bent hydrogel with 18-crown-6 ether, removes the K^+ ions, resulting in the dissociation of the G-quadruplex cross-linking units and the recovery of state i.

The preparation all of bilayer-hydrogel systems followed the same platform outlined in Figure 1, except that the compositions of the polymer mixtures comprising the respective bilayers were altered. The specific composition of the polymer mixtures used to assemble the different bilayer hydrogels are outlined in Figures 2a,c, 3a,b, and S4a (SI). In all of the bilayer hydrogel systems that were described, we used the T−A·T triplex units, rather than a simple duplex, as a common cross-linking element of the hydrogels and as a self-healing unit that combines the two layer of the hydrogel systems. We omitted the use of simple duplex bridging units and preferred the use of the T−A·T bridges due to the following reasons: (i) In order to generate the bilayer hydrogel structure, it is mandatory to introduce each of the mixtures as a solution that undergoes a transition into the hydrogel state in the mold. A simple duplex hydrogel cross-linking element would require the heating of the mixture to form the liquid state, prior to the introduction into the mold. For some of the

DOI: 10.1021/jacs.6b10458
J. Am. Chem. Soc. 2016, 138, 16112−16119

systems, e.g. pNIPAM hydrogel system, such heat treatment would lead to an adverse solidification of the mixture. For enzyme-triggered bilayer hydrogels, such thermal heating could deactivate the biocatalysts. (ii) The T−A·T cross-linking units permit the pH-triggered formation and separation of the triplex bridges. At pH 10.0, the hydrogel mixture is retained as a solution phase. The addition of the mixture to the first hydrogel layer, present in the mold, allows the separation of T−A·T triplex units at the hydrogel−solution boundary and, upon the rapid adjustment of the pH to 7.0, the gelation of the upper hydrogel layer with the concomitant bridging of the two hydrogel layers by the self-healing principle.

In the different bilayer hydrogel systems, described thus far, one of the hydrogel layers was subjected to an external trigger that resulted in a hydrogel layer of enhanced stiffness. The bending phenomenon was attributed to a stiffness-induced stress that was developed in one of the hydrogel layers. To emphasize the linkage between the stiffness and the stress of a layer, we refer to the Stoney relation, which formulates the relation between the stress of a layered system, the Young's modulus of the layer, and the length/width of the layer. Accordingly, we evaluated the Young's moduli values for all signal-triggered hydrogels used in the study, before and after affecting the stiffening stimuli (see Table S1, SI). Indeed, we find that stiffening of any of the hydrogels is accompanied by an increase in the Young's moduli of the systems, consistent with the development of a stress in the respective hydrogel layer. This qualitative evaluation of the bending process of the bilayer hydrogel structures was further addressed by developing a theoretical model for the triggered modulation of the shapes of the bilayer hydrogel systems.

To theoretically account for the experimentally found bending curvatures of the hydrogels, we developed a model that allows calculation of the bending radius from geometrical and stiffness considerations of the separated "free" hydrogel systems before incorporation into a bilayer hydrogel. The model considers the equilibrium curvature of the hydrogel bilayer as the minimum of an elastic free energy, representing the thermodynamically stable state. Solving the full elastic problem is a formidable task that moreover requires information on multiple system parameters. We simplify the system by considering the sum of two important elastic free energy terms, $E_{tot} = E_{ex} + E_b$, as parameters controlling the hydrogel stretching and hydrogel bending. These free energy terms account for the main deformations that the hydrogel undergoes when the two layers are coupled, compared with the same hydrogel layers when decoupled under the same solution conditions. For stretching (or compression), each of the two gel layers is penalized with an energy

$$E_{ex(n)} = 1/2Y_n(\delta_n/L_n)^2 L_n b c_n \quad (1)$$

where Y_n is the Young's modulus, δ_n (can be positive or negative in sign) is the deviation in hydrogel length from the equilibrium length (L_n) of the same hydrogel in the decoupled system, b is layer width, c_n is layer thickness, and $n = 1, 2$ is the bilayer index; see Figure 3d.

The second free energy term corresponds to hydrogel bending. Here we use the Canham−Helfrich−Evans theory,[36] which relates the bending energy with layer curvature as long as the layer is not too thick

$$E_{b(n)} = 1/2k_n L_n b(1/R_m)^2 \quad (2)$$

where R_m is the (average) hydrogel radius of curvature, defined here as

$$R_m = \frac{c_1 + c_2}{2} + \frac{(c_1 + c_2)(L_2 + \delta_2)}{(L_1 + \delta_1) - (L_2 + \delta_2)} \quad (3)$$

In eq 2, the bending modulus k can be shown theoretically to be $k = Yc^3/[a(1 - \nu^2)]$, where ν is the Poisson's ratio for the hydrogel (typically assumed to be 0.5) and a is a parameter related to the material structure and properties.[37] We find that choosing $a = 6$ results in good fits for all systems studied here. Finally, we also account for hydrogel thickness and Young's modulus variations due to hydrogel deformation compared with the values found at equilibrium with the following linear scaling for the Young's modulus, $Y_n = Y_{n,0} - Y_{n,0}(\delta_{n,theor}/4\delta_{n,exp})$, and for thickness $C_n = C_{n,exp} - (C_{n,exp} - C_{n,0})(\delta_{n,theor}/\delta_{n,exp})$. In these expressions, the subscript 0 represents the values prior to hydrogel bending, the subscript "theor" represents the deformation value if no variation in Y and C is assumed, while the subscript "exp" is the value reached in the experiment. The component δ_{exp} is taken as 0.001 m for $n = 1$ and 0.002 m for $n = 2$, while C_0 is taken as $C_{n,exp}$ + 0.0004 m for both $n = 1$, 2. Minimization of the elastic free energy E_{tot} allows us to derive the value of R_m at equilibrium. We find excellent agreement between the theoretical model and our experimental data (Figure 3e), suggesting that the two modes of deformation that are accounted for in the model are the most important and dictate the equilibrium structure. In order to test the robustness of the model, we compared predicted and experimental bending values, both within a given bilayer system, by changing hydrogel thicknesses, and across two hydrogel systems. The first system, as shown in Figure 2b, possessed a bilayer of T−A·T-cross-linked polyacrylamide (hydrogel I) and pNIPAM (hydrogel II). At 45 °C, the model predicted the radius of curvature to be 0.36 cm, which matched the experimental value of 0.36 cm. Upon increasing the thickness of both hydrogel layers (Figure S1, SI), both model and experiment indicated less bending and higher radius of curvature, with the theoretical radius of curvature value of 0.55 cm matching closely the experimental value of 0.57 cm.

In analyzing another bilayer system that displays two modes of bending, specifically pH-triggered and temperature-triggered bending, as shown in Figure 2d, we see that upon subjecting the bilayer hydrogel to solution at 45 °C, the model predicts a bending radius of 0.44 cm with an experimental value of 0.47 cm. Furthermore, as the solution returns to room temperature and the pH is changed from neutral to pH 5.0, we get a model radius of curvature fit of −1.2 cm, implying that bending is now in the opposite direction (bending toward the i-motif cross-linked hydrogel). We measured the experimental radius of curvature value to be −1.15 cm, thus demonstrating that our theoretical modeling allows us to predict and design bilayer systems using multiple bending triggers.

In the next phase, we attempted to use addressable chemical reactions on the asymmetric bilayer hydrogel to induce shape changes on the composite. In one system, we constructed a bilayer hydrogel composed of T−A·T-cross-linked polyacrylamide that is cooperatively stabilized by K^+ ion-stabilized G-quadruplex cross-linking units as hydrogel IV (polymer IV) (Figure 4a). The hydrogel I layer was composed of T−A·T-cross-linked polyacrylamide, polymer I. The association of hemin to the K^+ ion-stabilized G-quadruplex yields a hemin/G-quadruplex horseradish peroxidase-mimicking DNAzyme. This

DOI: 10.1021/jacs.6b10458
J. Am. Chem. Soc. 2016, 138, 16112−16119

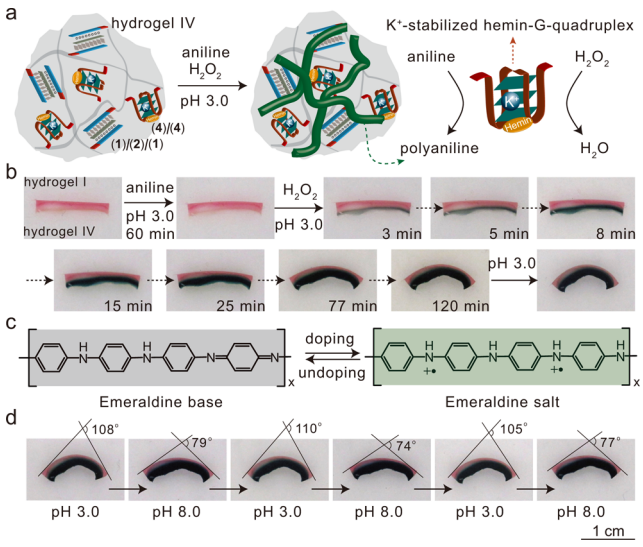

Figure 4. Synthesis of an asymmetric polyaniline-functionalized bilayer hydrogel and its reversible, switchable shape bending by the proton doping/undoping of polyaniline. (a) Deposition of polyaniline on a cooperatively cross-linked acrylamide copolymer using T−A·T [(**1**)/(**2**)/(**1**)] and hemin/G-quadruplex DNAzyme [(**4**)/(**4**)] bridges. (b) Time-dependent bending of an asymmetric bilayer hybrid hydrogel system consisting of the T−A·T [(**1**)/(**2**)/(**1**)]-cross-linked acrylamide copolymer (hydrogel I) and the T−A·T [(**1**)/(**2**)/(**1**)]- and hemin/G-quadruplex [(**4**)/(**4**)]-cross-linked acrylamide copolymer (hydrogel IV), upon the catalyzed deposition of polyaniline on the hydrogel IV layer. (c) Switchable pH-induced doping/undoping of polyaniline. (d) pH-stimulated, reversible bending of the polyaniline-modified bilayer hybrid hydrogel.

DNAzyme catalyzes the oxidation of aniline by H_2O_2 to form polyaniline.[38] Accordingly, hemin was incorporated in the G-quadruplex-cross-linked hydrogel IV domain of the bilayer composite with the vision that the dictated hemin/G-quadruplex-catalyzed oxidation of aniline in hydrogel IV will increase its stiffness and will result in the chemically induced bending of the bilayer hydrogel. Figure 4b demonstrates the time-dependent shape changes of the bilayer composite upon the asymmetric deposition of polyaniline on the domain of hydrogel IV. As the reaction proceeds, the negative curvature of the structure is more pronounced, consistent with the formation of a stiffer domain in hydrogel IV as polyaniline is deposited in this domain of the bilayer. The radius of the resulting curvature after deposition of polyaniline corresponds to 0.56 cm. The polyaniline deposited on the bilayer hydrogel structure is formed at pH 3.0, yielding the protonated emeraldine salt (dark green). That is, the stress being developed in the polyaniline-functionalized hydrogel may originate from the enhanced stiffness of the hydrogel IV domain and from cooperative stress affected by the electrostatic repulsive interactions of the positively charged protonated polyaniline chains.[39] Thus, by the reversible doping of the polyaniline to form the emeraldine salt (pH 3.0, dark green) and the undoping of the polyaniline (pH 8.0, black), the stress developed by the deposited polyaniline may switch between higher and lower values due to the existence or removal of the electrostatic repulsive interactions (Figure 4c). The pH-stimulated bending shapes of the polyaniline-functionalized bilayer hydrogel are depicted in Figure 4d. The protonated doped polyaniline hydrogel reveals a radius of curvature of 0.57 cm (angle between arms 105°−110°), whereas the undoped composite shows a radius of curvature of 0.68 cm (angle between arms 74°−79°), consistent with the enhanced electrostatic stress in the doped system. The pH-switchable shapes of the polyaniline-modified bilayer hydrogel are reversible. The results imply that a chemical reaction can change the shape of an asymmetric hydrogel structure, and the resulting new shape acts as mechanical "tweezers" upon doping and undoping of the structure.

Finally, the incorporation of enzymes into the asymmetric bilayer hydrogel composite enabled the switchable biocatalytic control of the shape of the hybrid structure (Figure 5). The

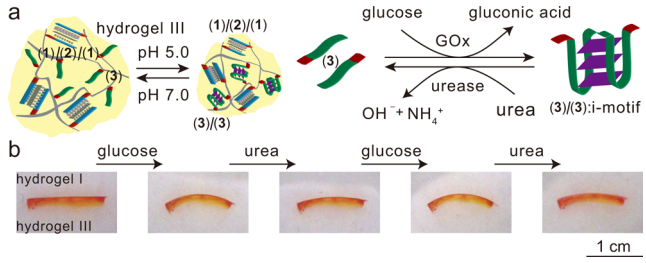

Figure 5. Switchable and reversible biocatalyzed bending of a bilayer hybrid asymmetric hydrogel system. (a) A pH-responsive acrylamide copolymer system, composed of the T−A·T [(**1**)/(**2**)/(**1**)] and i-motif subunits [(**3**)/(**3**)] as cross-linkers (hydrogel III), and the biocatalyzed, pH-stimulated control of the hydrogel stiffness by the enzymes glucose oxidase and urease being incorporated in the hydrogel. The glucose oxidase-mediated oxidation of glucose to gluconic acid acidifies the hydrogel, resulting in a hydrogel of enhanced stiffness due to the cooperative cross-linking of the hydrogel by T−A·T and i-motif bridges. Treatment of the hydrogel with urea results in the urease-induced neutralization of the system, leading to a hydrogel of lower stiffness, due to the separation of the i-motif cross-linking units. (b) Cyclic and reversible pH-stimulated bending of a bilayer glucose oxidase/urease-functionalized asymmetric hybrid system (hydrogel I/hydrogel III) upon treatment with glucose or urea.

polyacrylamide hydrogel III is composed of the polymer III, which results in the T−A·T triplex cross-linked hydrogel, and it is also modified by the cytosine-rich tethers [(**3**)]. While at pH 7.0 the tethers exist in a random coil structure, at pH 5.0 the tethers reconfigure into the i-motif structure that cooperatively increases the stiffness of the hydrogel (Figure 5a). Hydrogel I is composed of the T−A·T-cross-linked polyacrylamide hydrogels, and it lacks any additional cross-linking element. The two enzymes glucose oxidase (GOx) and urease were incorporated between hydrogel I and hydrogel III to form a sandwich structure. Accordingly, the GOx-catalyzed oxidation of glucose by O_2 to form gluconic acid is anticipated to acidify the hybrid bilayer, resulting in the enhanced stiffness introduced into hydrogel III through the formation of the i-motif bridges, leading to a negative bending of the composite. In turn, treatment of the bent hydrogel with urea results in neutralization of the system through the urease-catalyzed dissociation of urea. This process separates the i-motif cross-linking units, resulting in the release of the stress in hydrogel III and the recovery of the bilayer into the linear structure. Figure 5b depicts the reversible bending of the linear bilayer system and the recovery of the linear hybrid by the biocatalytic oxidation of glucose and biocatalyzed cleavage of urea by GOx and urease, respectively. The time-dependent pH changes induced by the bilayer hydrogel that includes the two enzymes, GOx and urease, upon the sequential addition of glucose/urea are depicted in Figure S5 (SI). After addition of glucose (70

DOI: 10.1021/jacs.6b10458
J. Am. Chem. Soc. 2016, 138, 16112−16119

mM), the pH of the system reached after ca. 80 min the value of 5.0 (capable of generating the i-motif structures) and after ca. 100 min leveled off to a value of pH 4.0, suggesting that glucose was consumed. Further addition of urea (50 mM) regenerated the system at pH 7.0, after ca. 50 min. Parallel stiffness measurements revealed that the Young's moduli of the hydrogel III in the hydrogel bilayer I/III changed from 0.83 to 1.23 KPa, consistent with the increased stiffness of hydrogel III as a result of the formation of the i-motif cross-linking bridges. Substitution of the Young's moduli changes of hydrogel I and III, upon the glucose-mediated acidification of the system, and the geometrical parameters of the bilayer hydrogel into the presented theoretical model suggests that the predicted radius of curvature of the bilayer hydrogel would be R_m = 0.97 cm. Indeed, the experimental value is R_m = 1.04 cm, in excellent agreement with the theoretically predicted value.

CONCLUSION

In conclusion, the present study has introduced DNA-based hydrogel composites as functional materials for controlling the reversible dynamic mechanical modulation of the shape of an asymmetric bilayer hydrogel composite. In contrast to previously reported organic/inorganic signal-triggered shape-modulated polymer matrices, the rich arsenal of stimuli-responsive DNA hydrogels provides diverse new means to design hydrogel materials exhibiting mechanically shape-modulated structures. Furthermore, the catalytic functions of the DNA components allow the dictated chemical deposition of auxiliary polymer matrices on the asymmetric hydrogel layers, which permit further control of the layer stiffness by doping/undoping processes. Specifically, we demonstrated the assembly of asymmetric linear bilayers of hydrogels cross-linked by T−A·T triplex bridges, using the self-healing principle. By the functionalization of one (or two) layers by stimuli-responsive units that control the stiffness (or stress) of the respective layers, negative or positive bending of the linear bilayer structures was demonstrated. The transitions between the curved and linear shapes of the bilayer hydrogel hybrids were reversible upon the application of trigger/counter-trigger stimuli. Different stimuli were applied to control the bending of the bilayer asymmetric hydrogel hybrids, and these included thermal, pH, and K^+ ion/crown ether stimuli. Also, the addressed chemical deposition of polyaniline within one of the hydrogel layers resulted in the permanent bending of the polyaniline-functionalized bilayer composite, and the pH-stimulated opening/closing of the bent hydrogel structure upon doping and undoping of the polyaniline adsorbate. Finally, by incorporation of two enzymes (GOx and urease) in the asymmetric bilayer structure, the biocatalyzed pH-driven bending of the hybrid hydrogel and its recovery to the linear structure were demonstrated. Important practical applications of stimuli-responsive asymmetric hydrogel composites exhibiting controlled shapes may be envisaged. These include the development of shaped, mechanically responsive sensors and the assembly of stimuli-responsive valves or actuators.

EXPERIMENTAL SECTION

DNA Sequences. The sequences involved in the study are (**1**), 5′-acrydite-TTC TTT TCT TTT CTT TTC TT-3′; (**2**), 5′-AAG AAA AGA AAA GAA AAG AA-3′; (**3**), 5′-acrydite-AAA CCC CTA ACC CC-3′; and (**4**), 5′-acrydite-AAG GGT TAG GG-3′.

Synthesis of the Acrylamide/Acrydite-Nucleic Acid Copolymers. A buffer solution (HEPES, 10 mM, $MgCl_2$, 100 mM, pH 7.0, 200 μL) that included 2.5% acrylamide and the acrydite-modified DNA strand (**1**) (1.2 mM) was prepared. Nitrogen was bubbled through the solution. Fifteen microliters of a 0.2 mL aqueous solution that included APS (20 mg) and TEMED (10 μL) was added to the mixture. The resulting solution was allowed to polymerize at room temperature for 5 min, and then, the solution was further polymerized at 4 °C for 12 h. The resulting copolymer was purified from unreacted monomer units, salts, and initiators, using a Microcon (Millipore) spin filter unit (MWCO 10 kDa). The purified polymer was removed from the filter and dried under a gentle nitrogen flow.

For other hydrogel systems, the procedures to prepare the copolymer chains were similar to the above-mentioned one, yet different monomers (acrylamide or NIPAM) and acrydite-modified DNA strands were used. Further details on the preparation of the polymers and their characterizations are provided in the Supporting Information.

Preparation of the Hybrid Asymmetric Bilayered Hydrogels. To form a linear-shaped T−A·T triplex cross-linked polyacrylamide/DNA hydrogel, the dried copolymer sample polymer I was dissolved in a 200 μL of HEPES buffer solution (HEPES, 10 mM, $MgCl_2$, 100 mM, pH 7.0) to yield a mixture containing 0.96 mM nucleic acid (**1**). To 20 μL of polymer I solution was added nucleic acid (**2**) (final concentration 0.48 mM) to form a polyacrylamide/DNA hydrogel based on the cross-linking by T−A·T triplex. A 0.8 μL portion of 25% ammonia solution was added to the hydrogel to dissolve it into solution, and 0.5 μL of SYBR Green I was introduced for the final staining of the resulting hydrogel. Then the solution was poured into a linear-shaped tetrafluoroethylene mold. A 2 μL portion of 5% acetic acid was added into the mold to neutralize the solution to a linear-shaped hydrogel.

The dried copolymer sample polymer II was also dissolved in a 200 μL HEPES buffer solution (HEPES, 10 mM, $MgCl_2$, 100 mM, pH 7.0) to yield a mixture containing 1.07 mM nucleic acid (**1**). To 50 μL of polymer II solution was added nucleic acid (**2**) (final concentration 0.53 mM) to form a pNIPAM/DNA hydrogel based on the cross-linking by T−A·T triplex. A 1 μL portion of 25% ammonia solution was added to the hydrogel to dissolve it into solution, and 1 μL of Gel Red was introduced for the final staining of the resulting hydrogel. Then the solution state was poured on top of the previously formed polyacrylamide/DNA hydrogel in the linear-shaped tetrafluoroethylene mold. After the addition of the liquefied mixture of the constituents of the upper hydrogel, the system was kept at room temperature for 30 min to allow the formation of the self-healing interface on top of the bottom hydrogel. Subsequently, 5 μL of 3% acetic acid aqueous solution was added to the upper quasi-liquid and the resulting neutralized system was allowed to form the bilayer hydrogel system for a time-interval of 5 h. After further incubation of the bilayer hydrogel overnight at 4 °C, the resulting linear-shaped T−A·T triplex cross-linked hybrid hydrogels were removed from the mold. It should be noted that we used SYBR Green I or Gel Red as DNA staining agents, rather than dye-labeled polymers, in order to eliminate possible interactions between the dye-labeled polymers and the hydrogel constituents, which could affect the stiffness properties of the hydrogels.

For the bending of the T−A·T triplex cross-linked hybrid hydrogels and the recovery to the linear shape, the linear-shaped structure was first immersed in a HEPES buffer solution (HEPES, 10 mM, $MgCl_2$, 100 mM, pH 7.0) and the solution was heated gradually up to 45 °C within 20 min. Then, the curved structure changed to a linear shape when the cell was allowed to cool down to room temperature within 2 h. It should be noted that the imaging of the structures was taken with buffer solution in the cell, unless otherwise noted.

Deposition of Polyaniline in the Hydrogel. After the formation of a hybrid asymmetric bilayered hydrogel (I and IV) in the mold, it was transferred into a HEPES buffer solution (HEPES, 10 mM, $MgCl_2$, 100 mM, pH 3.0) containing KCl (200 mM) and aniline (50 mM). After incubation for 1 h, H_2O_2 (final concentration 50 mM) was added to the buffer solution, which initiated the polymerization of aniline by the catalysis of hemin/G-quadruplex DNAzyme. After polymerization for 2 h, the formed polyaniline/hydrogels were

DOI: 10.1021/jacs.6b10458
J. Am. Chem. Soc. 2016, 138, 16112−16119

transferred into a HEPES buffer solution (HEPES, 10 mM, $MgCl_2$, 100 mM, pH 3.0). Doping and undoping of polyaniline/hydrogels composites were achieved by changing the pH of buffer solution to 3.0 or 8.0.

■ ASSOCIATED CONTENT

Supporting Information

The Supporting Information is available free of charge on the ACS Publications website at DOI: 10.1021/jacs.6b10458.

Materials, shaped hydrogel formation and triggered responsiveness, loading of the different nucleic acids tethers in the copolymer chains, NMR measurements, microindentation measurements (PDF)

■ AUTHOR INFORMATION

Corresponding Author

*willnea@vms.huji.ac.il

Notes

The authors declare no competing financial interest.

■ ACKNOWLEDGMENTS

This research is supported by the Israel Science Foundation. The imaging of the structures by Chang Liu is greatly acknowledged.

■ REFERENCES

(1) (a) Capadona, J. R.; Shanmuganathan, K.; Tyler, D. J.; Rowan, S. J.; Weder, C. *Science* **2008**, *319*, 1370−1374. (b) Hu, Z.; Zhang, X.; Li, Y. *Science* **1995**, *269*, 525−527.

(2) (a) Li, X.; Serpe, M. J. *Adv. Funct. Mater.* **2014**, *24*, 4119−4126. (b) Wu, Z. L.; Moshe, M.; Greener, J.; Therien-Aubin, H.; Nie, Z.; Sharon, E.; Kumacheva, E. *Nat. Commun.* **2013**, *4*, 1586.

(3) (a) Nath, U.; Crawford, B. C.; Carpenter, R.; Coen, E. *Science* **2003**, *299*, 1404−1407. (b) Harrington, M. J.; Razghandi, K.; Ditsch, F.; Guiducci, L.; Rueggeberg, M.; Dunlop, J. W.; Fratzl, P.; Neinhuis, C.; Burgert, I. *Nat. Commun.* **2011**, *2*, 337. (c) Fratzl, P.; Barth, F. G. *Nature* **2009**, *462*, 442−448.

(4) (a) Annabi, N.; Tamayol, A.; Uquillas, J. A.; Akbari, M.; Bertassoni, L. E.; Cha, C.; Camci-Unal, G.; Dokmeci, M. R.; Peppas, N. A.; Khademhosseini, A. *Adv. Mater.* **2014**, *26*, 85−124. (b) Hoare, T. R.; Kohane, D. S. *Polymer* **2008**, *49*, 1993−2007. (c) Randall, C. L.; Gultepe, E.; Gracias, D. H. *Trends Biotechnol.* **2012**, *30*, 138−146.

(5) (a) Calvert, P. *Adv. Mater.* **2009**, *21*, 743−756. (b) Majidi, C. *Soft Rob.* **2014**, *1*, 5−11.

(6) Dong, L.; Agarwal, A. K.; Beebe, D. J.; Jiang, H. *Nature* **2006**, *442*, 551−554.

(7) Richter, A.; Howitz, S.; Kuckling, D.; Arndt, K.-F. *Sens. Actuators, B* **2004**, *99*, 451−458.

(8) Stuart, M. A. C.; Huck, W. T. S.; Genzer, J.; Müller, M.; Ober, C.; Stamm, M.; Sukhorukov, G. B.; Szleifer, I.; Tsukruk, V. V.; Urban, M.; Winnik, F.; Zauscher, S.; Luzinov, I.; Minko, S. *Nat. Mater.* **2010**, *9*, 101−113.

(9) (a) Jiang, S.; Liu, F.; Lerch, A.; Ionov, L.; Agarwal, S. *Adv. Mater.* **2015**, *27*, 4865−4870. (b) Asoh, T.-a.; Matsusaki, M.; Kaneko, T.; Akashi, M. *Adv. Mater.* **2008**, *20*, 2080−2083. (c) Kim, J.; Hanna, J. A.; Hayward, R. C.; Santangelo, C. D. *Soft Matter* **2012**, *8*, 2375. (d) Kim, Y. S.; Liu, M.; Ishida, Y.; Ebina, Y.; Osada, M.; Sasaki, T.; Hikima, T.; Takata, M.; Aida, T. *Nat. Mater.* **2015**, *14*, 1002−1007.

(10) Motornov, M.; Sheparovych, R.; Lupitskyy, R.; MacWilliams, E.; Hoy, O.; Luzinov, I.; Minko, S. *Adv. Funct. Mater.* **2007**, *17*, 2307−2314.

(11) Yu, Y.; Nakano, M.; Ikeda, T. *Nature* **2003**, *425*, 145.

(12) Smela, E.; Inganas, O.; Lundstrom, I. *Science* **1995**, *268*, 1735−1738.

(13) Holmes, D. P.; Roché, M.; Sinha, T.; Stone, H. A. *Soft Matter* **2011**, *7*, 5188.

(14) (a) Therien-Aubin, H.; Wu, Z. L.; Nie, Z.; Kumacheva, E. *J. Am. Chem. Soc.* **2013**, *135*, 4834−4839. (b) Wei, Z. J.; Jia, Z.; Athas, J. M.; Wang, C. Y.; Raghavan, S. R.; Li, T.; Nie, Z. H. *Soft Matter* **2014**, *10*, 8157−8162.

(15) Maeda, S.; Hara, Y.; Sakai, T.; Yoshida, R.; Hashimoto, S. *Adv. Mater.* **2007**, *19*, 3480−3484.

(16) Wang, F.; Liu, X.; Willner, I. *Angew. Chem., Int. Ed.* **2015**, *54*, 1098−1129.

(17) Teller, C.; Willner, I. *Curr. Opin. Biotechnol.* **2010**, *21*, 376−391.

(18) Rosi, N. L.; Mirkin, C. A. *Chem. Rev.* **2005**, *105*, 1547−1562.

(19) Breaker, R. R.; Joyce, G. F. *Chem. Biol.* **1994**, *1*, 223−229.

(20) (a) Lu, C. H.; Willner, I. *Angew. Chem., Int. Ed.* **2015**, *54*, 12212−12235. (b) Liao, W. C.; Lu, C. H.; Hartmann, R.; Wang, F.; Sohn, Y. S.; Parak, W. J.; Willner, I. *ACS Nano* **2015**, *9*, 9078−9086.

(21) Balogh, D.; Aleman Garcia, M. A.; Albada, H. B.; Willner, I. *Angew. Chem., Int. Ed.* **2015**, *54*, 11652−11656.

(22) Freeman, R.; Liu, X.; Willner, I. *J. Am. Chem. Soc.* **2011**, *133*, 11597−11604.

(23) Xiong, X.; Wu, C.; Zhou, C.; Zhu, G.; Chen, Z.; Tan, W. *Macromol. Rapid Commun.* **2013**, *34*, 1271−1283.

(24) (a) Guo, W.; Lu, C. H.; Orbach, R.; Wang, F.; Qi, X. J.; Cecconello, A.; Seliktar, D.; Willner, I. *Adv. Mater.* **2015**, *27*, 73−78. (b) Hu, Y.; Lu, C.-H.; Guo, W.; Aleman-Garcia, M. A.; Ren, J.; Willner, I. *Adv. Funct. Mater.* **2015**, *25*, 6867−6874. (c) Hu, Y.; Guo, W.; Kahn, J. S.; Aleman-Garcia, M. A.; Willner, I. *Angew. Chem., Int. Ed.* **2016**, *55*, 4210−4214.

(25) Guo, W.; Qi, X. J.; Orbach, R.; Lu, C. H.; Freage, L.; Mironi-Harpaz, I.; Seliktar, D.; Yang, H. H.; Willner, I. *Chem. Commun.* **2014**, *50*, 4065−4068.

(26) Lu, C. H.; Guo, W.; Hu, Y.; Qi, X. J.; Willner, I. *J. Am. Chem. Soc.* **2015**, *137*, 15723−15731.

(27) Peng, L.; You, M.; Yuan, Q.; Wu, C.; Han, D.; Chen, Y.; Zhong, Z.; Xue, J.; Tan, W. *J. Am. Chem. Soc.* **2012**, *134*, 12302−12307.

(28) Ren, J.; Hu, Y.; Lu, C. H.; Guo, W.; Aleman-Garcia, M. A.; Ricci, F.; Willner, I. *Chem. Sci.* **2015**, *6*, 4190−4195.

(29) Li, J.; Zheng, C.; Cansiz, S.; Wu, C.; Xu, J.; Cui, C.; Liu, Y.; Hou, W.; Wang, Y.; Zhang, L.; Teng, I. t.; Yang, H.-H.; Tan, W. *J. Am. Chem. Soc.* **2015**, *137*, 1412−1415.

(30) Yang, H.; Liu, H.; Kang, H.; Tan, W. *J. Am. Chem. Soc.* **2008**, *130*, 6320−6321.

(31) Kahn, J. S.; Trifonov, A.; Cecconello, A.; Guo, W.; Fan, C.; Willner, I. *Nano Lett.* **2015**, *15*, 7773−7778.

(32) (a) Fahn, A.; Werker, E. *Seed Biology* **1972**, 151−221. (b) Fahn, A.; Zohary, M. *Phytomorphology* **1955**, *5*, 99.

(33) (a) Kim, J.; Hanna, J. A.; Byun, M.; Santangelo, C. D.; Hayward, R. C. *Science* **2012**, *335*, 1201−1205. (b) Ma, M.; Guo, L.; Anderson, D. G.; Langer, R. *Science* **2013**, *339*, 186−189. (c) Kohlmeyer, R. R.; Chen, J. *Angew. Chem., Int. Ed.* **2013**, *52*, 9234−9237.

(34) Armon, S.; Efrati, E.; Kupferman, R.; Sharon, E. *Science* **2011**, *333*, 1726−1730.

(35) Palleau, E.; Morales, D.; Dickey, M. D.; Velev, O. D. *Nat. Commun.* **2013**, *4*, 2257.

(36) (a) Helfrich, W. *Z. Naturforsch., C: J. Biosci.* **1973**, *28*, 693−703. (b) Evans, E. A. *Biophys. J.* **1974**, *14*, 923−931. (c) Canham, P. B. *J. Theor. Biol.* **1970**, *26*, 61−81.

(37) (a) Picas, L.; Rico, F.; Scheuring, S. *Biophys. J.* **2012**, *102*, L01−03. (b) Rawicz, W.; Olbrich, K. C.; McIntosh, T.; Needham, D.; Evans, E. *Biophys. J.* **2000**, *79*, 328−339. (c) *Faraday Discuss.* **2013**, *161*, 113−150.10.1039/C2FD90041F

(38) Lu, C. H.; Guo, W.; Qi, X. J.; Neubauer, A.; Paltiel, Y.; Willner, I. *Chem. Sci.* **2015**, *6*, 6659−6664.

(39) Lahav, M.; Durkan, C.; Gabai, R.; Katz, E.; Willner, I.; Welland, M. E. *Angew. Chem., Int. Ed.* **2001**, *40*, 4095−4097.